

Search for rare decay $J/\psi \rightarrow \phi e^+ e^-$

M. Ablikim¹, M. N. Achasov^{10,d}, S. Ahmed¹⁵, M. Albrecht⁴, M. Alekseev^{55A,55C}, A. Amoroso^{55A,55C}, F. F. An¹, Q. An^{52,42}, Y. Bai⁴¹, O. Bakina²⁷, R. Baldini Ferroli^{23A}, Y. Ban³⁵, K. Begzsuren²⁵, D. W. Bennett²², J. V. Bennett⁵, N. Berger²⁶, M. Bertani^{23A}, D. Bettoni^{24A}, F. Bianchi^{55A,55C}, E. Boger^{27,b}, I. Boyko²⁷, R. A. Briere⁵, H. Cai⁵⁷, X. Cai^{1,42}, A. Calcaterra^{23A}, G. F. Cao^{1,46}, S. A. Cetin^{45B}, J. Chal^{55C}, J. F. Chang^{1,42}, W. L. Chang^{1,46}, G. Chelkov^{27,b,c}, G. Chen¹, H. S. Chen^{1,46}, J. C. Chen¹, M. L. Chen^{1,42}, P. L. Chen⁵³, S. J. Chen³³, X. R. Chen³⁰, Y. B. Chen^{1,42}, W. Cheng^{55C}, X. K. Chu³⁵, G. Cibinetto^{24A}, F. Cossio^{55C}, H. L. Dai^{1,42}, J. P. Dai^{37,h}, A. Dbeyssi¹⁵, D. Dedovich²⁷, Z. Y. Deng¹, A. Denig²⁶, I. Denysenko²⁷, M. Destefanis^{55A,55C}, F. De Mori^{55A,55C}, Y. Ding³¹, C. Dong³⁴, J. Dong^{1,42}, L. Y. Dong^{1,46}, M. Y. Dong^{1,42,46}, Z. L. Dou³³, S. X. Du⁶⁰, P. F. Duan¹, J. Fang^{1,42}, S. S. Fang^{1,46}, Y. Fang¹, R. Farinelli^{24A,24B}, L. Fava^{55B,55C}, S. Fegan²⁶, F. Feldbauer⁴, G. Felici^{23A}, C. Q. Feng^{52,42}, E. Fioravanti^{24A}, M. Fritsch⁴, C. D. Fu¹, Q. Gao¹, X. L. Gao^{52,42}, Y. Gao⁴⁴, Y. G. Gao⁶, Z. Gao^{52,42}, B. Garillon²⁶, I. Garzia^{24A}, A. Gilman⁴⁹, K. Goetzen¹¹, L. Gong³⁴, W. X. Gong^{1,42}, W. Gradl²⁶, M. Greco^{55A,55C}, L. M. Gu³³, M. H. Gu^{1,42}, Y. T. Gu¹³, A. Q. Guo¹, L. B. Guo³², R. P. Guo^{1,46}, Y. P. Guo²⁶, A. Guskov²⁷, Z. Haddadi²⁹, S. Han⁵⁷, X. Q. Hao¹⁶, F. A. Harris⁴⁷, K. L. He^{1,46}, X. Q. He⁵¹, F. H. Heinsius⁴, T. Held⁴, Y. K. Heng^{1,42,46}, Z. L. Hou¹, H. M. Hu^{1,46}, J. F. Hu^{37,h}, T. Hu^{1,42,46}, Y. Hu¹, G. S. Huang^{52,42}, J. S. Huang¹⁶, X. T. Huang³⁶, X. Z. Huang³³, Z. L. Huang³¹, T. Hussain⁵⁴, W. Ikegami Andersson⁵⁶, M. Irshad^{52,42}, Q. Ji¹, Q. P. Ji¹⁶, X. B. Ji^{1,46}, X. L. Ji^{1,42}, H. L. Jiang³⁶, X. S. Jiang^{1,42,46}, X. Y. Jiang³⁴, J. B. Jiao³⁶, Z. Jiao¹⁸, D. P. Jin^{1,42,46}, S. Jin³³, Y. Jin⁴⁸, T. Johansson⁵⁶, A. Julin⁴⁹, N. Kalantar-Nayestanaki²⁹, X. S. Kang³⁴, M. Kavatsyuk²⁹, B. C. Ke¹, I. K. Keshk¹, T. Khan^{52,42}, A. Khoukaz⁵⁰, P. Kiese²⁶, R. Kiuchi¹, R. Kliemt¹¹, L. Koch²⁸, O. B. Kolcu^{45B,f}, B. Kopf⁴, M. Kornicer⁴⁷, M. Kuemmel⁴, M. Kuessner⁴, A. Kupsc⁵⁶, M. Kurth¹, R. S. Lange²⁸, P. Larin¹⁵, L. Lavezzi^{55C}, S. Leiber⁴, H. Leithoff²⁶, C. Li⁵⁶, Cheng Li^{52,42}, D. M. Li⁶⁰, F. Li^{1,42}, F. Y. Li³⁵, G. Li¹, H. B. Li^{1,46}, H. J. Li^{1,46}, J. C. Li¹, J. W. Li⁴⁰, K. J. Li⁴³, Kang Li¹⁴, Ke Li¹, Lei Li³, P. L. Li^{52,42}, P. R. Li^{46,7}, Q. Y. Li³⁶, T. Li³⁶, W. D. Li^{1,46}, W. G. Li¹, X. L. Li³⁶, X. N. Li^{1,42}, X. Q. Li³⁴, Z. B. Li⁴³, H. Liang^{52,42}, Y. F. Liang³⁹, Y. T. Liang²⁸, G. R. Liao¹², L. Z. Liao^{1,46}, J. Libby²¹, C. X. Lin⁴³, D. X. Lin¹⁵, B. Liu^{37,h}, B. J. Liu¹, C. X. Liu¹, D. Liu^{52,42}, D. Y. Liu^{37,h}, F. H. Liu³⁸, Fang Liu¹, Feng Liu⁶, H. B. Liu¹³, H. L. Liu⁴¹, H. M. Liu^{1,46}, Huanhuan Liu¹, Huihui Liu¹⁷, J. B. Liu^{52,42}, J. Y. Liu^{1,46}, K. Y. Liu³¹, Ke Liu⁶, L. D. Liu³⁵, Q. Liu⁴⁶, S. B. Liu^{52,42}, X. Liu³⁰, Y. B. Liu³⁴, Z. A. Liu^{1,42,46}, Zhiqing Liu²⁶, Y. F. Long³⁵, X. C. Lou^{1,42,46}, H. J. Lu¹⁸, J. G. Lu^{1,42}, Y. Lu¹, Y. P. Lu^{1,42}, C. L. Luo³², M. X. Luo⁵⁹, T. Luo^{9,j}, X. L. Luo^{1,42}, S. Lusso^{55C}, X. R. Lyu⁴⁶, F. C. Ma³¹, H. L. Ma¹, L. L. Ma³⁶, M. M. Ma^{1,46}, Q. M. Ma¹, X. N. Ma³⁴, X. Y. Ma^{1,42}, Y. M. Ma³⁶, F. E. Maas¹⁵, M. Maggiora^{55A,55C}, S. Maldaner²⁶, Q. A. Malik⁵⁴, A. Mangoni^{23B}, Y. J. Mao³⁵, Z. P. Mao¹, S. Marcello^{55A,55C}, Z. X. Meng⁴⁸, J. G. Messchendorp²⁹, G. Mezzadri^{24A}, J. Min^{1,42}, T. J. Min³³, R. E. Mitchell²², X. H. Mo^{1,42,46}, Y. J. Mo⁶, C. Morales Morales¹⁵, N. Yu. Muchnoi^{10,d}, H. Muramatsu⁴⁹, A. Mustafa⁴, S. Nakhoul^{11,g}, Y. Nefedov²⁷, F. Nerling^{11,g}, I. B. Nikolaev^{10,d}, Z. Ning^{1,42}, S. Nisar⁸, S. L. Niu^{1,42}, X. Y. Niu^{1,46}, S. L. Olsen⁴⁶, Q. Ouyang^{1,42,46}, S. Pacetti^{23B}, Y. Pan^{52,42}, M. Papenbrock⁵⁶, P. Patteri^{23A}, M. Pelizaeus⁴, J. Pellegrino^{55A,55C}, H. P. Peng^{52,42}, Z. Y. Peng¹³, K. Peters^{11,g}, J. Pettersson⁵⁶, J. L. Ping³², R. G. Ping^{1,46}, A. Pitka⁴, R. Poling⁴⁹, V. Prasad^{52,42}, H. R. Qi², M. Qi³³, T. Y. Qi², S. Qian^{1,42}, C. F. Qiao⁴⁶, N. Qin⁵⁷, X. S. Qin⁴, Z. H. Qin^{1,42}, J. F. Qiu¹, S. Q. Qu³⁴, K. H. Rashid^{54,i}, C. F. Redmer²⁶, M. Richter⁴, M. Ripka²⁶, A. Rivetti^{55C}, M. Rolo^{55C}, G. Rong^{1,46}, Ch. Rosner¹⁵, A. Sarantsev^{27,e}, M. Savri^{24B}, K. Schoenning⁵⁶, W. Shan¹⁹, X. Y. Shan^{52,42}, M. Shao^{52,42}, C. P. Shen², P. X. Shen³⁴, X. Y. Shen^{1,46}, H. Y. Sheng¹, X. Shi^{1,42}, J. J. Song³⁶, W. M. Song³⁶, X. Y. Song¹, S. Sosio^{55A,55C}, C. Sowa⁴, S. Spataro^{55A,55C}, F. F. Sui³⁶, G. X. Sun¹, J. F. Sun¹⁶, L. Sun⁵⁷, S. S. Sun^{1,46}, X. H. Sun¹, Y. J. Sun^{52,42}, Y. K. Sun^{52,42}, Y. Z. Sun¹, Z. J. Sun^{1,42}, Z. T. Sun¹, Y. T. Tan^{52,42}, C. J. Tang³⁹, G. Y. Tang¹, X. Tang¹, M. Tiemens²⁹, B. Tsednee²⁵, I. Uman^{45D}, B. Wang¹, B. L. Wang⁴⁶, C. W. Wang³³, D. Wang³⁵, D. Y. Wang³⁵, Dan Wang⁴⁶, H. H. Wang³⁶, K. Wang^{1,42}, L. L. Wang¹, L. S. Wang¹, M. Wang³⁶, Meng Wang^{1,46}, P. Wang¹, P. L. Wang¹, W. P. Wang^{52,42}, X. F. Wang¹, Y. Wang^{52,42}, Y. F. Wang^{1,42,46}, Z. Wang^{1,42}, Z. G. Wang^{1,42}, Z. Y. Wang¹, Zongyuan Wang^{1,46}, T. Weber⁴, D. H. Wei¹², P. Weidenkaff²⁶, S. P. Wen¹, U. Wiedner⁴, M. Wolke⁵⁶, L. H. Wu¹, L. J. Wu^{1,46}, Z. Wu^{1,42}, L. Xia^{52,42}, X. Xia³⁶, Y. Xia²⁰, D. Xiao¹, Y. J. Xiao^{1,46}, Z. J. Xiao³², Y. G. Xie^{1,42}, Y. H. Xie⁶, X. A. Xiong^{1,46}, Q. L. Xiu^{1,42}, G. F. Xu¹, J. J. Xu^{1,46}, L. Xu¹, Q. J. Xu¹⁴, X. P. Xu⁴⁰, F. Yan⁵³, L. Yan^{55A,55C}, W. B. Yan^{52,42}, W. C. Yan², Y. H. Yan²⁰, H. J. Yang^{37,h}, H. X. Yang¹, L. Yang⁵⁷, R. X. Yang^{52,42}, S. L. Yang^{1,46}, Y. H. Yang³³, Y. X. Yang¹², Yifan Yang^{1,46}, Z. Q. Yang²⁰, M. Ye^{1,42}, M. H. Ye⁷, J. H. Yin¹, Z. Y. You⁴³, B. X. Yu^{1,42,46}, C. X. Yu³⁴, J. S. Yu³⁰, J. S. Yu²⁰, C. Z. Yuan^{1,46}, Y. Yuan¹, A. Yuncu^{45B,a}, A. A. Zafar⁵⁴, Y. Zeng²⁰, B. X. Zhang¹, B. Y. Zhang^{1,42}, C. C. Zhang¹, D. H. Zhang¹, H. H. Zhang⁴³, H. Y. Zhang^{1,42}, J. Zhang^{1,46}, J. L. Zhang⁵⁸, J. Q. Zhang⁴, J. W. Zhang^{1,42,46}, J. Y. Zhang¹, J. Z. Zhang^{1,46}, K. Zhang^{1,46}, L. Zhang⁴⁴, S. F. Zhang³³, T. J. Zhang^{37,h}, X. Y. Zhang³⁶, Y. Zhang^{52,42}, Y. H. Zhang^{1,42}, Y. T. Zhang^{52,42}, Yang Zhang¹, Yao Zhang¹, Yu Zhang⁴⁶, Z. H. Zhang⁶, Z. P. Zhang⁵², Z. Y. Zhang⁵⁷, G. Zhao¹, J. W. Zhao^{1,42}, J. Y. Zhao^{1,46}, J. Z. Zhao^{1,42}, Lei Zhao^{52,42}, Ling Zhao¹, M. G. Zhao³⁴, Q. Zhao¹, S. J. Zhao⁶⁰, T. C. Zhao¹, Y. B. Zhao^{1,42}, Z. G. Zhao^{52,42}, A. Zhemchugov^{27,b}, B. Zheng⁵³, J. P. Zheng^{1,42}, W. J. Zheng³⁶, Y. H. Zheng⁴⁶, B. Zhong³², L. Zhou^{1,42}, Q. Zhou^{1,46}, X. Zhou⁵⁷, X. K. Zhou^{52,42}, X. R. Zhou^{52,42}, X. Y. Zhou¹, Xiaoyu Zhou²⁰, Xu Zhou²⁰, A. N. Zhu^{1,46}, J. Zhu³⁴, J. Zhu⁴³, K. Zhu¹, K. J. Zhu^{1,42,46}, S. Zhu¹, S. H. Zhu⁵¹, X. L. Zhu⁴⁴, Y. C. Zhu^{52,42}, Y. S. Zhu^{1,46}, Z. A. Zhu^{1,46}, J. Zhuang^{1,42}, B. S. Zou¹, J. H. Zou¹

(BESIII Collaboration)

¹ Institute of High Energy Physics, Beijing 100049, People's Republic of China² Beihang University, Beijing 100191, People's Republic of China³ Beijing Institute of Petrochemical Technology, Beijing 102617, People's Republic of China⁴ Bochum Ruhr-University, D-44780 Bochum, Germany⁵ Carnegie Mellon University, Pittsburgh, Pennsylvania 15213, USA

- ⁶ Central China Normal University, Wuhan 430079, People's Republic of China
- ⁷ China Center of Advanced Science and Technology, Beijing 100190, People's Republic of China
- ⁸ COMSATS Institute of Information Technology, Lahore, Defence Road, Off Raiwind Road, 54000 Lahore, Pakistan
- ⁹ Fudan University, Shanghai 200443, People's Republic of China
- ¹⁰ G.I. Budker Institute of Nuclear Physics SB RAS (BINP), Novosibirsk 630090, Russia
- ¹¹ GSI Helmholtzcentre for Heavy Ion Research GmbH, D-64291 Darmstadt, Germany
- ¹² Guangxi Normal University, Guilin 541004, People's Republic of China
- ¹³ Guangxi University, Nanning 530004, People's Republic of China
- ¹⁴ Hangzhou Normal University, Hangzhou 310036, People's Republic of China
- ¹⁵ Helmholtz Institute Mainz, Johann-Joachim-Becher-Weg 45, D-55099 Mainz, Germany
- ¹⁶ Henan Normal University, Xinxiang 453007, People's Republic of China
- ¹⁷ Henan University of Science and Technology, Luoyang 471003, People's Republic of China
- ¹⁸ Huangshan College, Huangshan 245000, People's Republic of China
- ¹⁹ Hunan Normal University, Changsha 410081, People's Republic of China
- ²⁰ Hunan University, Changsha 410082, People's Republic of China
- ²¹ Indian Institute of Technology Madras, Chennai 600036, India
- ²² Indiana University, Bloomington, Indiana 47405, USA
- ²³ (A)INFN Laboratori Nazionali di Frascati, I-00044, Frascati, Italy; (B)INFN and University of Perugia, I-06100, Perugia, Italy
- ²⁴ (A)INFN Sezione di Ferrara, I-44122, Ferrara, Italy; (B)University of Ferrara, I-44122, Ferrara, Italy
- ²⁵ Institute of Physics and Technology, Peace Ave. 54B, Ulaanbaatar 13330, Mongolia
- ²⁶ Johannes Gutenberg University of Mainz, Johann-Joachim-Becher-Weg 45, D-55099 Mainz, Germany
- ²⁷ Joint Institute for Nuclear Research, 141980 Dubna, Moscow region, Russia
- ²⁸ Justus-Liebig-Universitaet Giessen, II. Physikalisches Institut, Heinrich-Buff-Ring 16, D-35392 Giessen, Germany
- ²⁹ KVI-CART, University of Groningen, NL-9747 AA Groningen, The Netherlands
- ³⁰ Lanzhou University, Lanzhou 730000, People's Republic of China
- ³¹ Liaoning University, Shenyang 110036, People's Republic of China
- ³² Nanjing Normal University, Nanjing 210023, People's Republic of China
- ³³ Nanjing University, Nanjing 210093, People's Republic of China
- ³⁴ Nankai University, Tianjin 300071, People's Republic of China
- ³⁵ Peking University, Beijing 100871, People's Republic of China
- ³⁶ Shandong University, Jinan 250100, People's Republic of China
- ³⁷ Shanghai Jiao Tong University, Shanghai 200240, People's Republic of China
- ³⁸ Shanxi University, Taiyuan 030006, People's Republic of China
- ³⁹ Sichuan University, Chengdu 610064, People's Republic of China
- ⁴⁰ Soochow University, Suzhou 215006, People's Republic of China
- ⁴¹ Southeast University, Nanjing 211100, People's Republic of China
- ⁴² State Key Laboratory of Particle Detection and Electronics, Beijing 100049, Hefei 230026, People's Republic of China
- ⁴³ Sun Yat-Sen University, Guangzhou 510275, People's Republic of China
- ⁴⁴ Tsinghua University, Beijing 100084, People's Republic of China
- ⁴⁵ (A)Ankara University, 06100 Tandogan, Ankara, Turkey; (B)Istanbul Bilgi University, 34060 Eyup, Istanbul, Turkey; (C)Uludag University, 16059 Bursa, Turkey; (D)Near East University, Nicosia, North Cyprus, Mersin 10, Turkey
- ⁴⁶ University of Chinese Academy of Sciences, Beijing 100049, People's Republic of China
- ⁴⁷ University of Hawaii, Honolulu, Hawaii 96822, USA
- ⁴⁸ University of Jinan, Jinan 250022, People's Republic of China
- ⁴⁹ University of Minnesota, Minneapolis, Minnesota 55455, USA
- ⁵⁰ University of Muenster, Wilhelm-Klemm-Str. 9, 48149 Muenster, Germany
- ⁵¹ University of Science and Technology Liaoning, Anshan 114051, People's Republic of China
- ⁵² University of Science and Technology of China, Hefei 230026, People's Republic of China
- ⁵³ University of South China, Hengyang 421001, People's Republic of China
- ⁵⁴ University of the Punjab, Lahore-54590, Pakistan
- ⁵⁵ (A)University of Turin, I-10125, Turin, Italy; (B)University of Eastern Piedmont, I-15121, Alessandria, Italy; (C)INFN, I-10125, Turin, Italy
- ⁵⁶ Uppsala University, Box 516, SE-75120 Uppsala, Sweden
- ⁵⁷ Wuhan University, Wuhan 430072, People's Republic of China
- ⁵⁸ Xinyang Normal University, Xinyang 464000, People's Republic of China
- ⁵⁹ Zhejiang University, Hangzhou 310027, People's Republic of China
- ⁶⁰ Zhengzhou University, Zhengzhou 450001, People's Republic of China

^a Also at Bogazici University, 34342 Istanbul, Turkey

^b Also at the Moscow Institute of Physics and Technology, Moscow 141700, Russia

^c Also at the Functional Electronics Laboratory, Tomsk State University, Tomsk, 634050, Russia

^d Also at the Novosibirsk State University, Novosibirsk, 630090, Russia

^e Also at the NRC "Kurchatov Institute", PNPI, 188300, Gatchina, Russia

^f Also at Istanbul Arel University, 34295 Istanbul, Turkey

^g Also at Goethe University Frankfurt, 60323 Frankfurt am Main, Germany

^h Also at Key Laboratory for Particle Physics, Astrophysics and Cosmology, Ministry of Education; Shanghai Key Laboratory for Particle Physics and Cosmology; Institute of Nuclear and Particle Physics, Shanghai 200240, People's Republic of China

ⁱ Also at Government College Women University, Sialkot - 51310. Punjab, Pakistan.

^j Also at Key Laboratory of Nuclear Physics and Ion-beam Application (MOE) and Institute of Modern Physics, Fudan University, Shanghai 200443, People's Republic of China

Using a data sample of 448.1×10^6 $\psi(3686)$ events collected at $\sqrt{s} = 3.686$ GeV with the BESIII detector at the BEPCII, we search for the rare decay $J/\psi \rightarrow \phi e^+ e^-$ via $\psi(3686) \rightarrow \pi^+ \pi^- J/\psi$. No signal events are observed and the upper limit on the branching fraction is set to be $\mathcal{B}(J/\psi \rightarrow \phi e^+ e^-) < 1.2 \times 10^{-7}$ at the 90% confidence level, which is still about one order of magnitude higher than the Standard Model prediction.

PACS numbers: 13.20.Gd, 13.40.Ks

I. INTRODUCTION

The BESIII experiment has accumulated 4.48×10^8 $\psi(3686)$ events which is the largest $\psi(3686)$ data sample produced directly in e^+e^- annihilation in the world currently. By tagging the two soft pions in the decay of $\psi(3686) \rightarrow \pi^+ \pi^- J/\psi$, the final states from J/ψ decay can be well distinguished. This provides an almost background free sample to investigate the rare J/ψ decay, which may be sensitive to new physics. The rare decay $J/\psi \rightarrow \phi e^+ e^-$ is one particularly interesting example [1]. This decay channel occurs mainly through the three dynamic processes shown in Figs. 1(a)-(c). These include: (a) the leading-order electromagnetic (EM) process; (b) the EM and strong mixed loop process; and (c) the EM process proceeding through three virtual photons. In diagram (b), the non-perturbative strong loop can be treated as proceeding through intermediate mesons, as discussed in Ref. [1]. Within the framework of the Standard Model (SM), the partial widths from the leading EM and mixed loop processes are predicted to be at a level of 10^{-6} and 10^{-9} keV, respectively, corresponding to branching fractions at the order of 10^{-8} and 10^{-11} [1]. However, if there is a new particle involved in the intermediate process, such as a dark photon with a mass of several MeV/ c^2 or a glueball with certain quantum numbers, contribution from Fig. 1(b) can be enhanced greatly. Thus, any deviations from the predictions [1] would hint at the existence of new physics. Alternatively, if a positive result were obtained with a branching fraction in the expected range, this decay channel could be used to extract information of some interesting mesons such as $f_0(980)$ or $a_0(980)$ since their form factors are involved in the predictions.

Although BESIII has also available the currently world's largest data sample of directly produced J/ψ , this is not used in the present analysis due to badly-controlled background contamination from QED processes. In this work, we report on search for the rare

decay of $J/\psi \rightarrow \phi e^+ e^-$ via $\psi(3686) \rightarrow \pi^+ \pi^- J/\psi$.

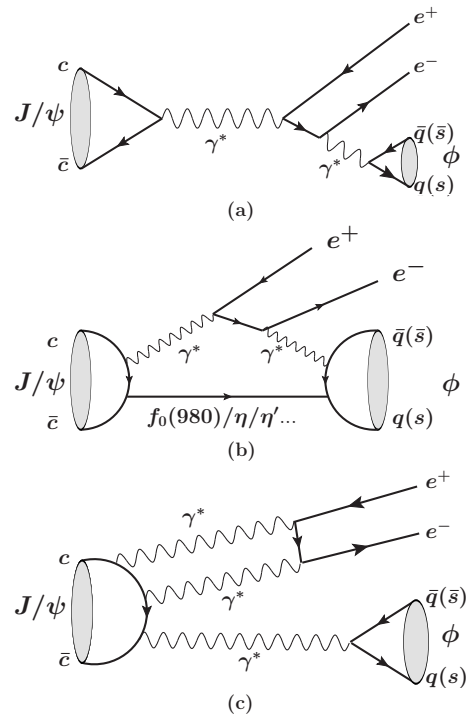


Figure 1. Feynman diagrams contributing to the decay $J/\psi \rightarrow \phi e^+ e^-$: (a) the leading-order EM process, (b) the EM and strong mixed loop process, and (c) the EM process proceeding through three virtual photons.

II. BESIII AND BEPCII

The BESIII detector [2] at the BEPCII e^+e^- collider is a major upgrade of the BESII experiment [3] at the Beijing Electron-Positron Collider (BEPC) and is optimized to study physics in the τ -charm energy region. The

design peak luminosity of BEPCII, $1.0 \times 10^{33} \text{ cm}^{-2}\text{s}^{-1}$ at a center-of-mass energy of 3773 MeV, was achieved in 2016. The BESIII detector, with a geometrical acceptance of 93% of the full solid angle, consists of the following five main components. (1) A small-celled multi-layer drift chamber (MDC) with 43 layers is used for charged track reconstruction and measurement of ionization energy loss (dE/dx). The average single-wire resolution is $135 \mu\text{m}$, and the momentum resolution for 1.0 GeV/ c charged particles in a 1 T magnetic field is 0.5%. The specific dE/dx resolution is 6% for electrons from Bhabha scattering. (2) A time-of-flight (TOF) system surrounds the MDC. This system is composed of a two-layer barrel, each layer consisting of 88 pieces of 5 cm thick and 2.4 m long plastic scintillators, as well as two end caps each with 96 fan-shaped, 5 cm thick, plastic scintillators. The time resolution is 80 ps in the barrel and 110 ps in the end caps, providing a K/π separation of more than 2σ for momenta up to 1.0 GeV/ c . (3) An electromagnetic calorimeter (EMC) is used to measure photon energies and consists of 6240 CsI(Tl) crystals in a cylindrically-shaped barrel and two end caps. For 1.0 GeV photons, the energy resolution is 2.5% in the barrel and 5% in the end caps, and the position resolution is 6 mm in the barrel and 9 mm in the end caps. (4) A superconducting solenoid magnet surrounding the EMC provides a 1 T magnetic field. (5) The muon chamber system is made of resistive plate chambers with 9 layers in the barrel and 8 layers in the end caps and is incorporated into the return iron yoke of the superconducting magnet. The global position resolution is about 2 cm.

Interactions within the BESIII detector are simulated by the GEANT4-based [4] simulation software BOOST [5], which includes: geometric and material descriptions of the BESIII detector; detector response and digitization models; and a record of detector running conditions and performances. The production of the $\psi(3686)$ resonance is simulated by the Monte Carlo (MC) generator KKMC [6], which incorporates the effects of the energy spread of the beam and initial-state radiation. Known decays are generated by EVTGEN [7] using the branching fractions quoted by the Particle Data Group (PDG) [8], and the remaining unknown decays are generated with the LUNDCHARM model [9].

In this analysis, the process $J/\psi \rightarrow \phi e^+ e^-$ is studied via $\psi(3686) \rightarrow \pi^+ \pi^- J/\psi$, and the ϕ meson is reconstructed using its decay to $K^+ K^-$. The transition $\psi(3686) \rightarrow \pi^+ \pi^- J/\psi$ is generated according to the results of an amplitude analysis as described in Ref. [10]. The process $J/\psi \rightarrow \phi e^+ e^-$ is generated according to the amplitude given in Ref. [1], in which the leading-order EM process is expected to be the dominant contribution according to the SM prediction. The spin correlation of J/ψ produced in the previous decay is considered as in Ref. [11]. The decay $\phi \rightarrow K^+ K^-$ is generated using a $\sin^2 \theta_K$ distribution, where θ_K is the helicity angle of the kaon in the center-of-mass system of the ϕ meson.

III. EVENT SELECTION

Charged tracks are reconstructed with MDC hits within the range $|\cos \theta| < 0.93$, where θ is the polar angle with respect to the electron beam direction. They are required to originate from the interaction region, defined as $R_{xy} < 1 \text{ cm}$ and $R_z < 10 \text{ cm}$, where R_{xy} and R_z are the projections of the distances from the closest approach of the tracks to the interaction point in the xy -plane and in the z -direction, respectively.

Particle identification (PID) probabilities for good charged tracks are calculated with the dE/dx and TOF measurements under the hypothesis that the track originated from a pion, kaon, proton or electron. For kaon candidates, we require that the probability for the kaon hypothesis is larger than the corresponding probability for the pion and proton hypotheses. For electron candidates, the probability for electron hypothesis is required to be larger than the probabilities for the pion and kaon hypotheses. To avoid contamination from pions, electron candidates must satisfy the additional requirement $E/p > 0.8$, where E and p represent the energy deposited in the EMC and the momentum of the electron, respectively.

For the two pions, no PID selection criterion is required. All pairs of opposite charged tracks with momentum less than 0.45 GeV/ c are assumed to be pions, and their recoil masses $M_{\pi^+ \pi^-}^{\text{rec}}$ are calculated and required to be within the range $(3.05, 3.15) \text{ GeV}/c^2$.

To improve the mass resolution and suppress backgrounds, an energy-momentum constrained kinematic fit (4C) to the initial beam four momentum is imposed on the selected charged tracks. The resulting χ_{4C}^2 of the kinematic fit is required to be less than 40. If more than one combination is found in an event, the combination with the least χ_{4C}^2 is retained for further analysis.

IV. ANALYSIS

The process $J/\psi \rightarrow \phi e^+ e^-$ is studied by examining the two-dimensional distribution of the $M_{\pi^+ \pi^-}^{\text{rec}}$ versus the invariant mass of the $K^+ K^-$ pair, $M_{K^+ K^-}$. Figure 2(a) shows the distribution for the signal MC sample, where the signal region (shown as a red solid box) is defined as $|M_{K^+ K^-} - M_\phi| < 0.010 \text{ GeV}/c^2$ and $|M_{\pi^+ \pi^-}^{\text{rec}} - M_{J/\psi}| < 0.007 \text{ GeV}/c^2$, where M_ϕ and $M_{J/\psi}$ are the nominal masses of ϕ and J/ψ mesons in taken from PDG [8], respectively. The five boxes with equal area around the signal region are selected as sideband regions, which are categorized into three types. The first type is used to estimate the background without a J/ψ in the intermediate state; the second one is for the estimation of the background without a ϕ in the intermediate state. These first two are shown as the pink dashed boxes and the green dashed double dotted box, respectively. The third type is for the estimation of the background that includes neither a J/ψ nor a ϕ in the intermediate

state, and is shown as blue dashed dotted boxes. Figure 2(b) shows the corresponding plot for the $\psi(3686)$ data sample. No events are observed in the signal region and two events are observed in the ϕ sideband. The non-flat non- ϕ background, mainly due to the threshold effect, is estimated by $\psi(3686) \rightarrow \pi^+\pi^-J/\psi$ with $J/\psi \rightarrow \phi\pi^+\pi^-$ and $\phi \rightarrow K^+K^-$. The scale factor is determined to be 0.8 for the background in the ϕ signal region to that in the ϕ sideband region. Therefore, the scaled background estimated by the sideband data is 1.6 ± 1.1 events. The projections of Fig. 2(b) on $M_{\pi^+\pi^-}^{\text{rec}}$ and $M_{K^+K^-}$ are shown in Figs. 3(a) and (b), respectively.

The backgrounds from $\psi(3686)$ decays are also studied with an inclusive MC sample of 506 million $\psi(3686)$ events. No events survive in the signal region, and only one event is found in the second type of sideband region. This event is from $\psi(3686) \rightarrow \pi^+\pi^-J/\psi$, $J/\psi \rightarrow K^+K^-\pi^0$, $\pi^0 \rightarrow \gamma e^+e^-$, which will not form a peak in ϕ signal region. In addition, the potential peaking backgrounds from $\psi(3686) \rightarrow \pi^+\pi^-J/\psi$ with $J/\psi \rightarrow \phi\eta/\pi^0$ and $\eta/\pi^0 \rightarrow \gamma e^+e^-$ are studied through exclusive MC events generated with a size corresponding to more than 100 times of that of data. The contribution from these channels is negligible.

Possible background sources from continuum processes are estimated with 44 pb^{-1} of data collected at a center-of-mass energy $\sqrt{s} = 3.65 \text{ GeV}$ [12], which is about one fifteenth of the integrated luminosity of the $\psi(3686)$ data. There are no events satisfying the above selection criteria, therefore we neglect the continuum background.

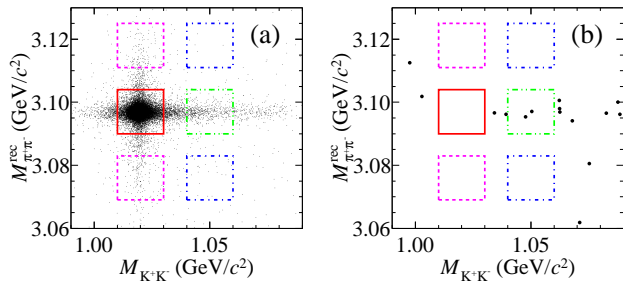


Figure 2. Distribution of $M_{\pi^+\pi^-}^{\text{rec}}$ versus $M_{K^+K^-}$ from (a) signal MC sample and (b) $\psi(3686)$ data. The signal region is defined as the solid box, and the three types of sideband regions (described in the text) are represented by the dashed, dashed double dotted, and dashed dotted boxes.

V. SYSTEMATIC UNCERTAINTIES

The systematic uncertainties originate mainly from the number of $\psi(3686)$ events, the tracking efficiency, the PID efficiency, the kinematic fit, the selection of the J/ψ and ϕ signal regions, background estimation, MC statistics, and the branching fractions of intermediate decays.

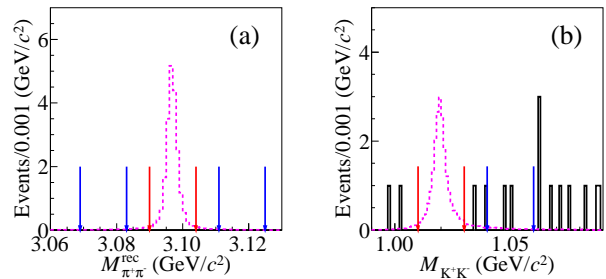


Figure 3. Distributions of (a) $M_{\pi^+\pi^-}^{\text{rec}}$ and (b) $M_{K^+K^-}$. The solid histograms represent the $\psi(3686)$ data and the dashed histograms represent signal MC with arbitrary scale. The region between the red arrows denotes the signal region, and the one(s) between the blue arrows denotes the sideband region(s).

These are discussed in detail in the following, and are summarized in Table I.

The uncertainty from the total number of $\psi(3686)$ events is estimated to be 0.7% [13].

The tracking efficiencies for π^\pm mesons have been studied with the process $\psi(3686) \rightarrow \pi^+\pi^-J/\psi$, $J/\psi \rightarrow \ell^+\ell^-$ ($\ell = e, \mu$). The difference in the efficiencies between data and MC simulation is 1.0% per pion [14]. The tracking efficiencies for K^\pm mesons as functions of transverse momentum have been studied with the process $J/\psi \rightarrow K_S^0 K^\pm \pi^\mp$, $K_S^0 \rightarrow \pi^+\pi^-$. The difference in the efficiencies between data and MC simulation is 1.0% per kaon [14]. The tracking efficiencies for e^\pm are obtained with a control sample of radiative Bhabha scattering $e^+e^- \rightarrow \gamma e^+e^-$ (including $J/\psi \rightarrow \gamma e^+e^-$) at the J/ψ resonance in Ref. [15]. The difference in tracking efficiencies between data and MC simulation is calculated bin-by-bin over the distribution of transverse momentum versus the polar angle of the lepton tracks. The uncertainty is determined to be 1.0% per electron/positron. The systematic uncertainties arising from the different charged tracks are summed linearly to be 6.0%.

High purity control samples of $e^+e^- \rightarrow \gamma e^+e^-$ and $J/\psi \rightarrow K^+K^-\pi^0$ have been selected to study the electron/positron and kaon PID uncertainty. The difference of PID efficiency between data and MC simulation is calculated in bins of momentum and $\cos\theta$. Averaged systematic uncertainties for electron/positron and kaon identification are obtained by weighting the difference with the events in each bin of momentum and $\cos\theta$ from the signal MC sample, and determined to be 0.4% per electron/positron and 0.8% per kaon. Adding these values linearly, the PID systematic uncertainty is determined to be 2.4%.

The systematic uncertainty of the 4C kinematic fit is studied using a control sample of $\psi(3686) \rightarrow \pi^+\pi^-J/\psi$ with $J/\psi \rightarrow \phi\pi^+\pi^-$, $\phi \rightarrow K^+K^-$. The efficiency difference between data and MC simulation with the $\chi_{4C}^2 < 40$ requirement is 3.3%, which is assigned as the systematic

uncertainty.

The uncertainty from the signal regions of $M_{K^+K^-}$ and $M_{\pi^+\pi^-}^{\text{rec}}$, due to their resolution difference between data and MC simulation, is studied by means of the control sample $\psi(3686) \rightarrow \pi^+\pi^- J/\psi$, $J/\psi \rightarrow \phi\pi^+\pi^-$, $\phi \rightarrow K^+K^-$. The efficiency differences in the $M_{K^+K^-}$ and $M_{\pi^+\pi^-}^{\text{rec}}$ signal regions between data and MC simulation are 0.2% and 1.8%, respectively. Adding them in quadrature yields 1.8%, which is taken as the systematic uncertainty.

The uncertainty on the background estimation is studied by an alternative estimation of the scale factor (0.74), estimated using the inclusive MC sample instead of data. The difference between the resulting upper limits is taken as the systematic uncertainty, which is 1.5%.

The uncertainty of the detection efficiency attributed to the limited size of the MC sample, 0.4%, is taken as the systematic uncertainty from MC statistics.

To estimate the uncertainty from the model used to simulate the $J/\psi \rightarrow \phi e^+e^-$ decay, we generated a MC sample based on the phase-space assumption. The difference between the efficiencies determined from the MC sample described in Sec. II and the phase space MC sample is 10.7%. We take half of the difference (5.4%) as the systematic uncertainty from MC modeling.

In the determination of the upper limit on the branching fraction of the process of interest, we have accounted for the branching fractions of $\psi(3686) \rightarrow \pi^+\pi^- J/\psi$ and $\phi \rightarrow K^+K^-$ by taking the values given by the PDG [8]. The uncertainties of these cited values are taken as a source of systematic uncertainty, which are 0.9% and 1.0%, respectively.

The total systematic uncertainty, Δ_{sys} , is calculated by adding the uncertainties from all sources in quadrature.

Table I. Summary of relative systematic uncertainties (in %).

Sources	Uncertainty
$N_{\psi(3686)}^{\text{tot}}$	0.7
Tracking	6.0
PID	2.3
Kinematic fit	3.3
Signal region	1.8
Background estimation	1.5
MC statistics	0.4
MC modeling	5.4
$\mathcal{B}(\psi(3686) \rightarrow \pi^+\pi^- J/\psi)$	0.9
$\mathcal{B}(\phi \rightarrow K^+K^-)$	1.0
Total	9.5

VI. RESULT

Since no candidate events are observed in the signal region and 1.6 ± 1.1 background events are estimated,

the upper limit on the number of $\psi(3686) \rightarrow \pi^+\pi^- J/\psi$ events with $J/\psi \rightarrow \phi e^+e^-$ is set to be 1.31 at the 90% confidence level (CL) using the Feldman-Cousins [16] method with the assumption of a Poisson process.

After taking into account the systematic uncertainty [17], the upper limit of the branching fraction of $J/\psi \rightarrow \phi e^+e^-$ is calculated with

$$\mathcal{B}(J/\psi \rightarrow \phi e^+e^-) < \frac{N^{\text{up}} \times (1 + N^{\text{up}} \times \Delta_{\text{sys}}^2/2)}{N_{\psi(3686)}^{\text{tot}} \times \epsilon \times \prod \mathcal{B}_i}, \quad (1)$$

where $N_{\psi(3686)}^{\text{tot}}$ is the number of $\psi(3686)$ events, $\prod \mathcal{B}_i$ represents the branching fraction product $\mathcal{B}(\psi(3686) \rightarrow \pi^+\pi^- J/\psi) \times \mathcal{B}(\phi \rightarrow K^+K^-)$ and ϵ is the detection efficiency, which is $(14.31 \pm 0.05)\%$ determined by MC simulations as described in Sec. II. Table II summarizes the various values that were used as input to Eq. (1). We find an upper limit on the branching fraction of the $J/\psi \rightarrow \phi e^+e^-$ process at the 90% CL of

$$\mathcal{B}(J/\psi \rightarrow \phi e^+e^-) < 1.2 \times 10^{-7}.$$

Table II. Input values used to obtain the upper limit on the branching fraction of $J/\psi \rightarrow \phi e^+e^-$. N^{obs} , N^{bkg} and N^{up} represent the number of observed events, background events, and the upper limit on the number of observed events, respectively.

Item	Value
$N_{\psi(3686)}^{\text{tot}}$	$(448.1 \pm 2.9) \times 10^6$
N^{obs}	0
N^{bkg}	1.6 ± 1.1
$N^{\text{up}}(90\% \text{ CL})$	1.31
ϵ	$(15.13 \pm 0.05)\%$
$\mathcal{B}(\psi(3686) \rightarrow \pi^+\pi^- J/\psi)$	$(34.49 \pm 0.30)\%$
$\mathcal{B}(\phi \rightarrow K^+K^-)$	$(48.9 \pm 0.5)\%$
Δ_{sys}	9.5%
$\mathcal{B}(J/\psi \rightarrow \phi e^+e^-)$	$< 1.2 \times 10^{-7}$

VII. SUMMARY

Using the 448.1×10^6 $\psi(3686)$ events collected with the BESIII detector, we report a search for the rare decay $J/\psi \rightarrow \phi e^+e^-$ via $\psi(3686) \rightarrow \pi^+\pi^- J/\psi$. No signal events are observed and the upper limit of the branching fraction for this decay is calculated to be $\mathcal{B}(J/\psi \rightarrow \phi e^+e^-) < 1.2 \times 10^{-7}$ by the Feldman-Cousins method at the 90% CL, which is one order of magnitude higher than the prediction in Ref. [1]. Our result shows that, even if there are new particles involved in the Fig. 1(b) process, their contributions will not be too large, and the masses of the possible existing new particles or their coupling information to vector mesons (J/ψ and ϕ) can also be constrained.

VIII. ACKNOWLEDGEMENTS

The BESIII collaboration thanks the staff of BEPCII and the IHEP computing center for their strong support. This work is supported in part by National Key Basic Research Program of China under Contract No. 2015CB856700; National Natural Science Foundation of China (NSFC) under Contracts Nos. 11575077, 11475090, 11235011, 11335008, 11425524, 11625523, 11635010, 11735014, 11835012; the Outstanding Youth project of Natural Science Foundation of Hunan Province; the Chinese Academy of Sciences (CAS) Large-Scale Scientific Facility Program; Joint Large-Scale Scientific Facility Funds of the NSFC and CAS under Contracts Nos. U1532257, U1532258, U1732263, U1832207; CAS Key Research Program of Frontier Sciences under Contracts Nos. QYZDJ-SSW-SLH003,

QYZDJ-SSW-SLH040; 100 Talents Program of CAS; IN-PAC and Shanghai Key Laboratory for Particle Physics and Cosmology; German Research Foundation DFG under Contract No. Collaborative Research Center CRC 1044; Istituto Nazionale di Fisica Nucleare, Italy; Koninklijke Nederlandse Akademie van Wetenschappen (KNAW) under Contract No. 530-4CDP03; Ministry of Development of Turkey under Contract No. DPT2006K-120470; National Science and Technology fund; The Knut and Alice Wallenberg Foundation (Sweden) under Contract No. 2016.0157; The Swedish Research Council; U. S. Department of Energy under Contracts Nos. DE-FG02-05ER41374, DE-SC-0010118, DE-SC-0012069; University of Groningen (RuG) and the Helmholtzzentrum für Schwerionenforschung GmbH (GSI), Darmstadt.

-
- [1] X. D. Guo, S. R. Xue, H. W. Ke, X. Q. Li, Q. Zhao, *Chin. Phys. C* **40**, 073104 (2016).
- [2] M. Ablikim *et al.* [BESIII Collaboration], *Nucl. Instrum. Meth. A* **614**, 345 (2010).
- [3] J. Z. Bai *et al.* [BES Collaboration], *Nucl. Instrum. Meth. A* **344**, 319 (1994); **458**, 627 (2001).
- [4] S. Agostinelli *et al.* [GEANT4 Collaboration], *Nucl. Instrum. Meth. A* **506**, 250 (2003).
- [5] Z. Y. Deng *et al.*, *High Energy Physics & Nuclear Physics* **30**, 371 (2006).
- [6] S. Jadach, B. F. L. Ward, and Z. Was, *Comput. Phys. Commun.* **130**, 260 (2000); *Phys. Rev. D* **63**, 113009 (2001).
- [7] R. G. Ping, *Chin. Phys. C* **32**, 599 (2008); D. J. Lange, *Nucl. Instrum. Meth. A* **462**, 152 (2001).
- [8] M. Tanabashi *et al.* [Particle Data Group], *Phys. Rev. D* **98**, 030001 (2018).
- [9] J. C. Chen, G. S. Huang, X. R. Qi, D. H. Zhang, Y. S. Zhu, *Phys. Rev. D* **62**, 034003 (2000); R. L. Yang, R. G. Rong and D. Chen, *Chin. Phys. Lett.* **31**, 061301 (2014).
- [10] M. Ablikim *et al.* [BES Collaboration], *Phys. Rev. D* **62**, 032002 (2000).
- [11] M. Ablikim *et al.* [BESIII Collaboration], arxiv:1809.00635.
- [12] M. Ablikim, *et al.* [BESIII Collaboration], *Chin. Phys. C* **37**, 123001 (2013).
- [13] M. Ablikim *et al.* [BESIII Collaboration], *Chin. Phys. C* **42**, 023001 (2018).
- [14] M. Ablikim *et al.* [BESIII Collaboration], *Phys. Rev. D* **83**, 112005 (2011).
- [15] M. Ablikim *et al.* [BESIII Collaboration], *Phys. Rev. D* **89**, 092008 (2014).
- [16] G. J. Feldman and R. D. Cousins, *Phys. Rev. D* **57**, 3873 (1998).
- [17] R. D. Cousins and V. L. Highland, *Nucl. Instrum. Meth. A* **320**, 331 (1992).